

## Formation of a Highly Ordered Colloidal Microstructure upon Flow Cessation from High Shear Rates

Robert J. Butera

*DuPont Marshall Laboratory, Philadelphia, Pennsylvania 19146*

Michael S. Wolfe

*DuPont CR&D, Experimental Station, Wilmington, Delaware 19898*

Jonathan Bender and Norman J. Wagner

*Center for Molecular and Engineering Thermodynamics, Department of Chemical Engineering,  
University of Delaware, Newark, Delaware 19716*

(Received 28 May 1996)

A model suspension of charged colloidal spheres exhibits anomalous modulus relaxations upon flow cessation from the shear-thickened state. Small angle neutron scattering (SANS) measurements indicate the development of a metastable crystalline state upon flow cessation from a disordered, shear-thickened state. The metastable state consists of a random stacking of tightly packed hcp planes of particles lying in the shear velocity-vorticity plane. These measurements suggest that the apparently disordered shear-thickened state may contain a high degree of latent order not apparent in the SANS measurements during flow. [S0031-9007(96)01057-5]

PACS numbers: 82.70.Dd, 61.12.Ex, 83.50.By, 83.70.Hq

Much of the current research on colloid rheology is aimed at understanding the nature of colloidal microstructures generated during flow. In particular, many investigations focus on shear-induced ordering, disordering, and shear thickening in concentrated suspensions (for example, see early work from Hoffmann [1], Ackerson and Clark [2], as well as recent investigations of Laun *et al.* [3], Chen *et al.* [4], and Bender and Wagner [5]). The present experimental work was initiated in an effort to explain the relaxation of moduli and structure from the shear-thickened state of an electrostatically stabilized acrylic latex dispersion in H<sub>2</sub>O that exhibits reversible and continuous shear thickening [6]. Through the use of small-strain oscillatory shear experiments after flow cessation from the shear-thickened state we found evidence of a long-lived structure induced during shear thickening. This induced structure can persist longer than 800 sec, depending on the strength of the electrostatic repulsion acting between the particles. Neutron scattering was performed on samples of this latex exchanged into D<sub>2</sub>O as a means to discern the structural details leading to this anomalous relaxation behavior. Although the shear modulus was shifted somewhat upon exchange into D<sub>2</sub>O, the exchanged sample exhibited a similar anomalous decay of the elastic modulus upon flow cessation from high shear rates. The scattering spectra revealed a surprising microstructure transition underlying this relaxation, namely, the formation of a highly ordered, metastable state immediately upon cessation of flow. The results indicate that the decay observed in the oscillatory shear experiments corresponds to a "melting" of this induced ordered state. This novel observation suggests the existence of some latent order in the shear-thickened

state that can guide the formation of this highly ordered, metastable colloidal crystal.

The latex used in this study has a composition of 60 wt.% butyl acrylate, 35 wt.% acrylonitrile, and 5 wt.% methacrylic acid with a particle diameter of 370 nm (narrow distribution), and was produced via emulsion polymerization in deionized water using sodium dodecyl sulfate as the surfactant. Rheological data were collected using a Rheometrics RFSII Fluids Spectrometer fitted with either Couette or cone and plate geometry. Rheological characterization of the sample after flow cessation was performed by first exposing the sample to the prescribed steady shear rate for 1 min and then, upon cessation of flow, immediately starting a small-strain oscillatory shear experiment at 10 rad/sec. The oscillatory data were collected every 15 sec.

Samples used for the neutron scattering experiments were prepared by exchanging most of the original H<sub>2</sub>O with D<sub>2</sub>O to provide contrast and reduce incoherent scattering. The rheology of similar samples in H<sub>2</sub>O has been previously reported [6]. The exchange was accomplished by diluting the original sample with an equal weight of D<sub>2</sub>O, centrifuging, then removing an equivalent weight of supernatant to restore the sample to the original solids weight fraction, and then resuspending the latex. The composition of the continuous medium after completing the exchange process was 66% D<sub>2</sub>O/34% H<sub>2</sub>O. The average particle size of the sample after this procedure was found to be identical (within experimental error) to that of the original sample. Electrostatic stabilization was effected via neutralization of the acid functionality of the latex using aqueous NH<sub>4</sub>OH as the neutralizing agent. The surface charge

density in these acid functionalized lattices corresponds directly to the degree of neutralization of the particles; thus, the surface charge can be controlled through the  $\text{NH}_4\text{OH}$  concentration. The data presented here are for a sample at solids volume fraction of 48% and 100% neutralization.

Flow small-angle neutron scattering (SANS) measurements were performed on the NG3 small angle instrument at NIST. The flow cell geometry consists of a quartz Couette cell with the beam orthogonal to the rotation axis. The cell was configured with a 0.488 mm gap. A wavelength of 18 Å with a spread of 14.7% was used throughout. The detector to sample distance was set at 13 m. Standard NIST data reduction techniques were used to reduce the data to absolute units [7].

The viscosity vs shear rate data shown in Fig. 1 demonstrate the complexity of the steady shear viscosity of the neutralized latex. At low shear rates the characteristic strong shear thinning behavior expected from an electrostatically stabilized latex sample at high volume fraction is observed. Note that this behavior is entirely reversible upon ramping up or down the shear rate. At higher shear rates a transition in behavior is evinced as a shoulder in the flow curve, followed by further shear thinning. This regime corresponds to strong shear thickening in the sample in  $\text{H}_2\text{O}$  [6]. The lack of clear shear thickening in the sample in  $\text{D}_2\text{O}$  may be a consequence of wall slip, and is currently under investigation.

Small-strain oscillatory shear measurements after flow cessation determined the time necessary for the sample's shear modulus (and hence microstructure) to recover. Figure 2 shows the change in elastic modulus as a function of time after cessation of flow at shear rates in the high shear as well as in the shear thinning region. Although not shown, the loss modulus  $G''$  always decreases upon flow cessation regardless of the steady shear rate, and is always less than the elastic modulus  $G'$ . Upon relaxation from a preshear rate of  $0.1 \text{ sec}^{-1}$  (which is in the low shear thinning region) the data show the expected behavior; the modulus rapidly increases as a function of time after flow cessation to its equilibrium value of  $230 \text{ dyn/cm}^2$ . This is expected for a weak shear that disrupts the rest fluid structure, which then rebuilds upon flow cessation. When

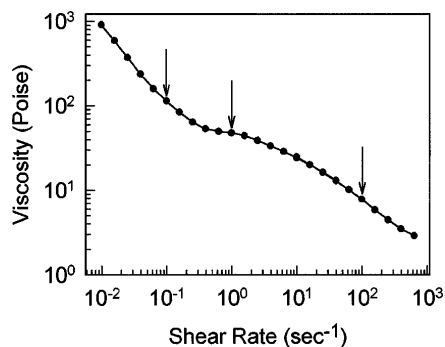


FIG. 1. Latex rheology in  $\text{D}_2\text{O}$ , at  $\phi = 0.48$  and 100% neutralization (arrows indicate shear rates used for modulus relaxation experiments).

a shear rate near the “shoulder” in the flow curve is used ( $1 \text{ sec}^{-1}$ ), the modulus after flow cessation is somewhat higher than the equilibrium value, gradually relaxing toward the equilibrium value. When substantially higher preshear rates are applied, the elastic modulus upon flow cessation is substantially larger than at equilibrium. It decays, but is still far higher than its equilibrium value even after 15 min. It should be noted that upon weak shearing the sample returns to its equilibrium fluid structure and modulus values, indicating the metastability of the induced elasticity. This same pattern of modulus relaxation is clearly evident in the sample in  $\text{H}_2\text{O}$ , where the anomalous behavior is only observed upon relaxation from a steady, shear-thickened flow [6]. The lack of shear thickening in the sample in  $\text{D}_2\text{O}$  may be a consequence of wall slip at the higher stresses.

Figures 3 and 4 show the SANS patterns obtained for two shear flows and the corresponding relaxations upon flow cessation for the sample in  $\text{D}_2\text{O}$ . The relaxation spectra are averaged over 10 min of collection time. For the sample in the shear thinning regime [Fig. 3(a)] a Debye-Scherrer ring with only very weak hexagonal ordering is observed. Upon relaxation [Fig. 3(b)], the sample returned to its rest state, which exhibits negligible ordering. Increasing the shear rate [to  $400 \text{ sec}^{-1}$ , Fig. 4(a)] reduces the amount of order present. However, immediately upon flow cessation a rather remarkable ordering becomes apparent. As seen in Fig. 4(b), Bragg spots appear and persist indefinitely, at the expense of the Debye-Scherrer ring. Visual observation through the quartz cell showed that, upon flow cessation, the sample instantly transformed from its usual milky white appearance to a highly iridescent green color superimposed on the milky white background, indicating a high degree of order. This state was observed to be metastable in that any significant amount of strain ( $\approx 10$ ) would “melt” the sample back to its original milky white state. However, gentle oscillations of the shear cell did not destroy the iridescence, suggesting that the low amplitude mechanical oscillatory measurements after flow would not disrupt the induced structure. Indeed, operation in the linear regime of  $\leq 1\%$  strain enabled modulus measurements on this microstructure without destabilizing it.

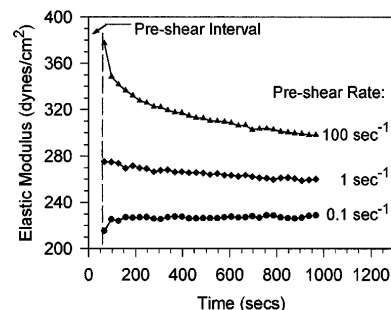


FIG. 2. Latex rheology in  $\text{D}_2\text{O}$ , at  $\phi = 0.48$ : elastic modulus at 10 rad/sec as a function of time after flow cessation from the indicated shear rates.

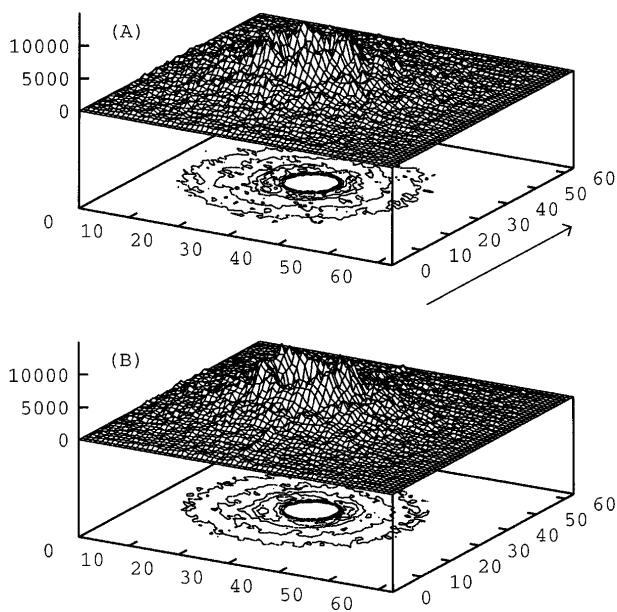


FIG. 3. SANS intensity patterns with the velocity axis indicated by the arrow and the orthogonal axis the vorticity axis of the flow: (a) under shear at  $0.4 \text{ sec}^{-1}$ ; (b) at rest after  $0.4 \text{ sec}^{-1}$ .

Additional SANS experiments on the latex sample in  $\text{H}_2\text{O}$  show the same qualitative behavior, but the large incoherent scattering obscures many details evident in the patterns taken on dispersions in  $\text{D}_2\text{O}$ .

As recently derived by Loose and Ackerson [8], the structure of the highly ordered state can be described by stacking sequences of planes of hexagonally close packed (hcp) particles. The magnitude of the positions for the

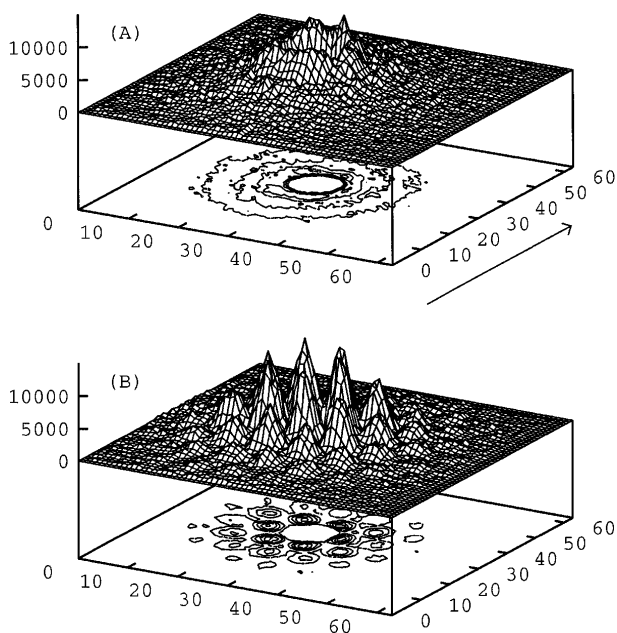


FIG. 4. SANS intensity patterns with the velocity axis indicated by the arrow and the orthogonal axis the vorticity axis of the flow: (a) under shear at  $400 \text{ sec}^{-1}$ ; (b) at rest after  $400 \text{ sec}^{-1}$ .

TABLE I. SANS peak positions.

Shell No.	$q \text{ (1/\AA)}$	$q/q_0$	$q/q_0 \text{ (theory)}$
1	0.00208	1	1
2	0.00330	1.59	$\sqrt{3} \approx 1.73$
3	0.00434	2.09	2
4	0.00523	2.52	$\sqrt{7} \approx 2.65$
5	0.00617	2.97	3
6	0.00719	3.46	$2\sqrt{3} \approx 3.46$

Bragg spots for the first few orders are given in Table I below, along with the predictions for randomly stacked hcp planes. The high degree of organization evident in the patterns suggests the hcp planes are highly organized with respect to the flow field, but the presence of the inner ring indicates that the hcp planes are stacked more or less randomly [8].

Note that the value of the 1st shell, or  $q_0 = 2.08 \times 10^{-3} \text{ \AA}^{-1}$ , is larger than the expected value of  $1.70 \times 10^{-3} \text{ \AA}^{-1}$ , as predicted by assuming fcc packing with stacking faults for these 370 nm diameter particles at 48% by volume. Indeed, this value suggests that the particles within the layers are touching, which would necessitate that the layers are actually farther apart in the shear gradient direction (which may explain some of the discrepancies observed in the Bragg peak positions). This microstructure (see Fig. 5) would presumably permit the layers to slide over one another more easily under steady shear as has previously been observed [4,9,10]; however, note that the data in Figs. 3(a) and 4(a) show that this structure does not exist under steady shear for our system.

The latex suspensions in  $\text{H}_2\text{O}$  [6] show a reversible shear-thickening behavior seen previously in both near hard-sphere silica and sterically stabilized-PMMA suspensions. Shear-induced order and disorder have been reported in many systems under a variety of conditions. However, this is the first report of such a highly organized *metastable* structure induced by *relaxation* from a flowing system. Indeed, such order is seldom, if ever, achieved under normal crystallization conditions in colloidal fluids. Further, this structure arises by the relaxation of a system driven far from equilibrium, i.e., the shear-thickened state.

The seemingly anomalous modulus relaxations observed in the dynamic mechanical measurements can be readily

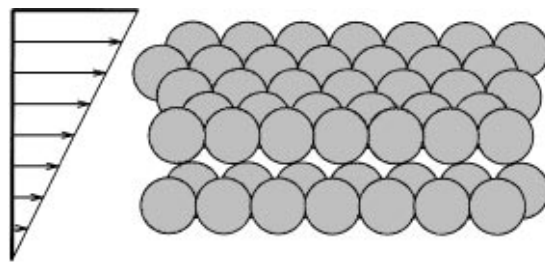


FIG. 5. Sketch of the structure of the metastable crystalline state deduced from the SANS data for the sample relaxed from the shear-thickened state.

interpreted in terms of this metastable ordering. The metastable crystalline lattice structure should exhibit a higher modulus at the test frequency than an equivalent fluid or even polycrystalline structure due to the long range order present in the crystalline solid. The SANS measurements (as well as the optical iridescence) provided the key information for understanding this peculiar rheology. However, the detailed mechanism for inducing this highly organized structure remains a mystery.

Clearly, the colloidal microstructure at high shear rates is qualitatively different than at lower shear rates, as evidenced by this anomalous relaxation behavior. In the suspension in H<sub>2</sub>O, this clearly correlates with the onset of shear thickening. The nature of the shear-thickened state is an active area of research in colloid rheology and has been studied both experimentally [3,5,11,12] and by simulation [13,14] and has been the subject of correlation and phenomenological modeling [15,16]. What is apparent is that in the shear-thickened state hydrodynamic lubrication forces “bind” particles into “hydroclusters” under flow, leading to the large increases in viscosity. Under certain conditions, these clusters can grow to span the flow cell, leading to dramatic changes in rheological properties. What remains unknown are the detailed structure of these hydroclusters and their extent and scaling with the applied field. The experimental observations presented here provide one clue as to the nature of this state; the structure observed in the ordered crystal obtained upon relaxation most probably reflects some latent order present in the shear-thickened state.

Financial support for this research was provided through the NSF (CTS-9158164) and DuPont. We acknowledge W. Graham of DuPont for synthesis of the latex samples and W. Kernick III for assistance with the SANS measurements. This material is based upon activities supported by the NSF under Agreement No. DMR-

9122444. We acknowledge the support of the NIST, U.S. Department of Commerce, in providing the facilities used for the SANS experiments.

- 
- [1] R. L. Hoffmann, *Trans. Soc. Rheol.* **16**, 155 (1972).
  - [2] B. J. Ackerson and N. A. Clark, *Phys. Rev. A* **30**, 906 (1984).
  - [3] H. M. Laun, R. Bung, S. Hess, W. Loose, K. Hahn, E. Hadicke, R. Hingmann, F. Schmidt, and P. Lindner, *J. Rheol.* **36**, 743 (1992).
  - [4] L. B. Chen, B. J. Ackerson, and C. F. Zukoski, *J. Rheol.* **38**, 193–216 (1994).
  - [5] J. W. Bender and N. J. Wagner, “Reversible Shear Thickening in Monodisperse and Bidisperse Colloidal Dispersions,” *J. Rheol.* (to be published).
  - [6] R. Butera, M. S. Wolfe, J. W. Bender, and N. J. Wagner, “Shear Thickening in an Electrostatically Stabilized Colloidal Suspension: Relaxation from the Shear Thickened State” (to be published).
  - [7] J. Barker, S. Krueger, and B. Hammouda, *SANS Manuals* (NIST, Gaithersburg, MD, 1993).
  - [8] W. Loose and B. J. Ackerson, *J. Chem. Phys.* **101**, 7211 (1994).
  - [9] H. Versmold, *Phys. Rev. Lett.* **75**, 763–766 (1995).
  - [10] C. Dux, H. Versmold, V. Reus, T. Zemb, and P. Lindner, “Neutron Diffraction from Shear Ordered Colloidal Dispersions” (to be published).
  - [11] P. D’Haene, J. Mewis, and G. G. Fuller, *J. Colloid Interface Sci.* **156**, 350–358 (1993).
  - [12] J. W. Bender and N. J. Wagner, *J. Colloid Interface Sci.* **172**, 171–184 (1995).
  - [13] J. F. Brady and G. Bossis, *Annu. Rev. Fluid Mech.* **20**, 111 (1988).
  - [14] T. Phung, Ph.D. thesis, Cal. Tech., 1994.
  - [15] H. A. Barnes, *J. Rheol.* **33**, 329–366 (1989).
  - [16] W. H. Boersma, J. Laven, and H. N. Stein, *AIChE J.* **36**, 321 (1990).